Electronic Supplementary Information (ESI) †

# Supported binary $CuO_x$−Pt catalysts with high activity and thermal stability for the combustion of $NH_3$ as a carbon-free energy source

Saaya Kiritoshi, [a] Takeshi Iwasa, [b] Kento Araki, [a] Yusuke Kawabata, [a] Tetsuya Taketsugu,[b] Satoshi Hinokuma [ac*] and Masato Machida [a]

[a] Field of Environmental Chemistry and Materials, Division of Materials Science and Chemistry, Faculty of Advanced Science and Technology, 2-39-1 Kurokami, Chuo-ku, Kumamoto 860-8555, Japan. E-mail: hinokuma@kumamoto-u.ac.jp.

[b] Department of Chemistry, Faculty of Science, Hokkaido University, Sapporo 060-0810, Japan.

[c] International Research Organization for Advanced Science and Technology, Kumamoto University, Japan.

**Figure captions**

**Figure S1.** Pt−$PtO_x$ phase equilibrium calculated from thermodynamics with HSC Chemistry 9 (Outotec Research Oy, Pori, Finland). Calculation condition: mol fraction of $PtO_{2(s)}$:$O_{2(g)}$:$N_{2(g)}$ = 0.001:20:80, pressure of 1 bar, temperature from 25 to 1000 °C.

**Figure S2.** XRD patterns of catalysts supported on 3A2S before and after thermal aging 900 °C for 100 h in air.

**Figure S3.** XRD patterns of catalysts supported on $Al_2O_3$ and CuO before and after thermal aging 900 °C for 100 h in air.

**Figure S4.** XRD patterns of catalysts supported on $SiO_2$ before and after thermal aging 900 °C for 100 h in air.

**Figure S5.** HAADF-STEM image and EDS mapping analysis of $CuO_x$/Pt/$SiO_2$(900 °C). Red, green, and blue points denote the Pt-L, Cu-K, and Si-K fluorescence lines.

**Figure S6.** Product selectivities for catalytic $NH_3$ combustion over catalysts supported on 3A2S. Reaction conditions: 1.0% $NH_3$, 1.5% $O_2$, $\lambda = 2$, He balance, $W/F = 5.0 \times 10^{-4}$ g min $cm^{-3}$.

**Figure S7.** Product selectivities for catalytic $NH_3$ combustion over catalysts supported on $Al_2O_3$. Reaction conditions: 1.0% $NH_3$, 1.5% $O_2$, $\lambda = 2$, He balance, $W/F = 5.0 \times 10^{-4}$ g min $cm^{-3}$.

**Figure S8.** Product selectivities for catalytic $NH_3$ combustion over catalysts. Reaction conditions: 1.0% $NH_3$, 1.5% $O_2$, $\lambda = 2$, He balance, W/F = $5.0 \times 10^{-4}$ g min $cm^{-3}$.

**Figure S9.** Product selectivities for catalytic $NH_3$ combustion over catalysts supported on $SiO_2$. Reaction conditions: 1.0% $NH_3$, 1.5% $O_2$, $\lambda = 2$, He balance, W/F = $5.0 \times 10^{-4}$ g min $cm^{-3}$.

**Figure S10.** Product selectivities for the $NH_3$–NO–$O_2$ reaction over supported catalysts before and after thermal aging. Reaction conditions: 0.8% $NH_3$, 0.2% NO, 1.4% $O_2$, He balance, W/F = $5.0 \times 10^{-4}$ g min $cm^{-3}$.

**Figure S11.** Correlation between $NH_3$ combustion activity ($T_{10}$) and Pt particle size for catalysts supported on $Al_2O_3$ before and after thermal aging. Pt particle size was estimated from the XRD line broadening method through the Scherrer equation.

**Figure S12.** Correlation between $NH_3$ combustion activity ($T_{10}$) and Pt particle size for catalysts supported on $SiO_2$ before and after thermal aging. Pt particle size was estimated from the XRD line broadening method through the Scherrer equation.

**Figure S13.** $NH_3$-TPD profiles of supported catalysts before and after thermal aging. 5% $NH_3$/He, 10 °C $min^{-1}$, m/z value of 15.

**Figure S14.** NO-TPD profiles of supported catalysts before and after thermal aging. 1% NO/He, 10 °C $min^{-1}$, m/z value of 30.

**Figure S15.** Product selectivities for the catalytic combustion of $NH_3$ ($NH_3$–$O_2$) over CuO (Wako Pure Chemicals), $Cu_2O$ (Wako Pure Chemicals), metallic Cu (CuO reduced at 400 °C for 30 min in 5% $H_2$/He). Reaction conditions: 1.0% $NH_3$, 1.5% $O_2$ ($\lambda = 2$), He balance, W/F = $5.0 \times 10^{-4}$ g·min·$cm^{-3}$.

**Figure S16.** XRD patterns of CuO (Wako Pure Chemicals) and $Cu_2O$ (Wako Pure Chemicals) before and after the reaction. Reaction conditions: 1.0% $NH_3$, 1.5% $O_2$ ($\lambda$ = 2.0), He balance and W/F = $5.0 \times 10^{-4}$ g·min·cm$^{-3}$.

## Materials and methods

*Calculation formulae of concentration ratios*

For $NH_3$ combustive decomposition, the concentration ratios were calculated using the following formulae:

$$NH_3 = [NH_{3out}]/[NH_{3in}],$$

$$N_2O = 2[N_2O_{out}]/[NH_{3in}],$$

$$NO = [NO_{out}]/[NH_{3in}],$$

$$N_2 = 2[N_{2out}]/[NH_{3in}],$$

where $[NH_{3in}]$ is the inlet $NH_3$ concentration (1.0%) and $[NH_{3out}]$, $[N_2O_{out}]$, $[NO_{out}]$ and $[N_{2out}]$ are the outlet gas concentrations. The $N_2O$ and $N_2$ concentration ratios were doubled as 2 mol of nitrogen was present. The formulae were approximated based on the hypothesis that the volume of the gas mixture before and after the reaction remained the same.

**Table S1.** Catalytic properties of supports and supported catalysts before and after thermal aging at 900 for 100 h in air

| Catalyst | Phase | $T_{10}$ [a] / °C | $T_{90}$ [a] / °C | Selectivity at $T_{90}$ [a] / % | | $S_{BET}$ / $m^2 \cdot g^{-1}$ | Pt particle size / nm | | Desorbed gas [d] / $\mu mol \cdot m^{-2}$ | |
|---|---|---|---|---|---|---|---|---|---|---|
| | | | | $N_2O$ | NO | | [b] XRD | [c] pulsed CO | $NH_3$ | NO |
| 3A2S | 3A2S | 576 | | | | 43 | | | | |
| $CuO_x$/3A2S | CuO/3A2S | 292 | 484 | <1 | 3 | 32 | | | 1.8 | 0.80 |
| Pt/3A2S | Pt/3A2S | 191 | 299 | 21 | <1 | 41 | | | | |
| $CuO_x$/Pt/3A2S | CuO/Pt/3A2S | 210 | 356 | 8 | 2 | 32 | | 18 | | |
| $CuO_x$/Pt/3A2S(900 °C) | $CuAl_2O_4$/Pt/3A2S | 203 | 344 | 10 | 1 | 27 | | 50 | | |
| $CuO_x$/Pt/3A2S(1000 °C) | $CuAl_2O_4$/Pt/3A2S | 258 | 398 | 3 | 2 | | | 66 | | |
| Pt/$CuO_x$/3A2S | Pt/CuO/3A2S | 213 | 337 | 7 | <1 | 50 | | | | |
| Pt/$CuO_x$/3A2S(900 °C) | Pt/$CuAl_2O_4$/3A2S | 241 | 405 | 8 | 3 | 40 | | | | |
| $CuO_x$−Pt/3A2S | CuO−Pt/3A2S | 255 | 345 | 4 | 1 | 50 | | | | |
| $CuO_x$−Pt/3A2S(900 °C) | $CuAl_2O_4$−Pt/3A2S | 252 | 421 | 6 | 3 | 40 | | | | |

[a] Temperature at which $NH_3$ conversion reached 10% and 90%. [b] Calculated from XRD line broadening method. [c] Calculated from pulsed CO chemisorption. [d] Estimated by $NH_3$- and NO-TPD ranging from 50 °C to 500 °C.

**Table S2.** Catalytic properties of supports and supported catalysts before and after thermal aging at 900 for 100 h in air

| Catalyst | Phase | $T_{10}$ [a] / °C | $T_{90}$ [a] / °C | Selectivity at $T_{90}$ [a] / % | | $S_{BET}$ / $m^2 \cdot g^{-1}$ | Pt particle size / nm | | Desorbed gas [d] / $\mu mol \cdot m^{-2}$ | |
|---|---|---|---|---|---|---|---|---|---|---|
| | | | | $N_2O$ | NO | | [b] XRD | [c] pulsed CO | $NH_3$ | NO |
| $Al_2O_3$ | γ-$Al_2O_3$ | 536 | 818 | <1 | 22 | 173 | | | | |
| $CuO_x/Al_2O_3$ | $CuAl_2O_4$/γ-$Al_2O_3$ | 303 | 476 | 6 | 2 | 149 | | | 1.3 | 0.050 |
| $CuO_x/Al_2O_3$(900 °C) | $CuAl_2O_4$/α, γ-$Al_2O_3$ | 295 | 450 | 8 | 1 | 102 | | | 0.4 | 0.063 |
| $Pt/Al_2O_3$ | Pt/γ-$Al_2O_3$ | 188 | 289 | 19 | <1 | 156 | 11 | 11 | 0.6 | 0.051 |
| $Pt/Al_2O_3$(900 °C) | Pt/γ, θ-$Al_2O_3$ | 213 | 266 | 12 | <1 | 99 | 31 | [e] n. d. | 2.0 | 0.140 |
| $CuO_x/Pt/Al_2O_3$ | $CuAl_2O_4$/Pt/γ-$Al_2O_3$ | 189 | 278 | 13 | <1 | 139 | 15 | 5 | 1.6 | 0.064 |
| $CuO_x/Pt/Al_2O_3$(900 °C) | $CuAl_2O_4$/Pt/α-$Al_2O_3$ | 220 | 339 | 13 | 1 | 14 | 33 | 176 | 1.5 | 0.444 |
| $CuO_x/Pt/Al_2O_3$(1000 °C) | $CuAl_2O_4$/Pt/α-$Al_2O_3$ | 204 | 310 | 13 | <1 | 10 | 35 | [e] n. d. | | |
| $CuO_x/Pt/\alpha$-$Al_2O_3$ | CuO/Pt/α-$Al_2O_3$ | 193 | 298 | 20 | 1 | 6 | 28 | | | |
| $CuO_x/Pt/\alpha$-$Al_2O_3$(900 °C) | CuO/Pt/α-$Al_2O_3$ | 198 | 475 | 4 | 10 | 4 | 33 | | | |
| $Pt/CuO_x/Al_2O_3$ | | 188 | 279 | 16 | <1 | 129 | 31 | 5 | | |
| $Pt/CuO_x/Al_2O_3$(900 °C) | $Pt/CuAl_2O_4/\alpha$-$Al_2O_3$ | 207 | 290 | 13 | <1 | 25 | 34 | 20 | | |
| $CuO_x$−$Pt/Al_2O_3$ | | 202 | 311 | 14 | 2 | 142 | 27 | | | |
| $CuO_x$−$Pt/Al_2O_3$(900 °C) | $CuAl_2O_4$−Pt/α-$Al_2O_3$ | 201 | 302 | 13 | <1 | 47 | 34 | | | |
| CuO + $Pt/Al_2O_3$ | | 184 | 253 | 17 | <1 | | | | | |
| $CuAl_2O_4$ + $Pt/Al_2O_3$ | | 198 | 284 | 20 | <1 | | | | | |
| $CuO_x/Al_2O_3$ + $Pt/Al_2O_3$ | | 197 | 270 | 15 | <1 | | | | | |
| Pt/CuO | | 284 | 396 | 7 | 1 | | | | | |

[a] Temperature at which $NH_3$ conversion reached 10% and 90%. [b] Calculated from XRD line broadening method. [c] Calculated from pulsed CO chemisorption. [d] Estimated by $NH_3$- and NO-TPD ranging from 50 °C to 500 °C. [e] The amount of CO chemisorption was not detected (n. d.).

**Table S3.** Catalytic properties of supports and supported catalysts before and after thermal aging at 900 for 100 h in air

| Catalyst | Phase | $T_{10}$ | $T_{90}$ | Selectivity at $T_{90}$ [a] / % | | $S_{BET}$ | Pt particle size / nm | | Desorbed gas [d] / μmol·m$^{-2}$ | |
|---|---|---|---|---|---|---|---|---|---|---|
| | | [a] / °C | [a] / °C | $N_2O$ | NO | / m$^2$·g$^{-1}$ | [b] XRD | [c] pulsed CO | $NH_3$ | NO |
| $SiO_2$ | $SiO_2$ | 527 | | | | 184 | | | | |
| $CuO_x/SiO_2$ | $CuO/SiO_2$ | 334 | 490 | 1 | 2 | 177 | | | 0.1 | 0.017 |
| $Pt/SiO_2$ | $Pt/SiO_2$ | 174 | 238 | 18 | <1 | 183 | 12 | | | |
| $CuO_x/Pt/SiO_2$ | $CuO/Pt/SiO_2$ | 234 | 316 | 7 | <1 | 182 | 13 | [e] n. d. | | |
| $CuO_x/Pt/SiO_2$(900 °C) | $CuO/Pt/SiO_2$ | 301 | 456 | <1 | 3 | 81 | 24 | [e] n. d. | | |
| $CuO_x/Pt/SiO_2$(1000 °C) | $CuO/Pt/SiO_2$ | 305 | 488 | 1 | 2 | 26 | 19 | [e] n. d. | | |
| $Pt/CuO_x/SiO_2$ | $PtO_2/CuO/SiO_2$ | 265 | 341 | 2 | <1 | 177 | 24 | | | |
| $Pt/CuO_x/SiO_2$(900 °C) | $Pt/CuO/SiO_2$ | 329 | 464 | 1 | 3 | 126 | 30 | | | |
| $CuO_x$−$Pt/SiO_2$ | $CuO−PtO_2/SiO_2$ | 311 | 392 | 2 | 3 | 173 | 22 | | | |
| $CuO_x$−$Pt/SiO_2$(900 °C) | $CuO−Pt/SiO_2$ | 322 | 496 | <1 | 4 | 100 | 32 | | | |

[a] Temperature at which $NH_3$ conversion reached 10% and 90%. [b] Calculated from XRD line broadening method. [c] Calculated from pulsed CO chemisorption. [d] Estimated by $NH_3$- and NO-TPD ranging from 50 °C to 500 °C. [e] The amount of CO chemisorption was not detected (n. d.).

**Table S4.** Adsorption energy ($E_{ads}$) between $NH_3$ and $Pt_{13}$ and/or $Pt_{20}$ clusters (Pt−N), and bond distances of N−H in $NH_3$ adsorbed on $Pt_{13}$ and/or $Pt_{20}$ obtained by the DFT computations

| Entry | Pt−N $E_{ads}$ / eV | N−H bond distance / Å |
|---|---|---|
| $Pt_{13}$ | | |
| vertex | 2.0456446 | 1.0262, 1.0262, 1.0302 |
| $Pt_{20}$ | | |
| vertex | 1.7915936 | 1.0266, 1.0270, 1.0274 |
| edge | 1.6096250 | 1.0266, 1.0267, 1.0281 |
| atop | 1.2762246 | 1.0270, 1.0282, 1.0295 |

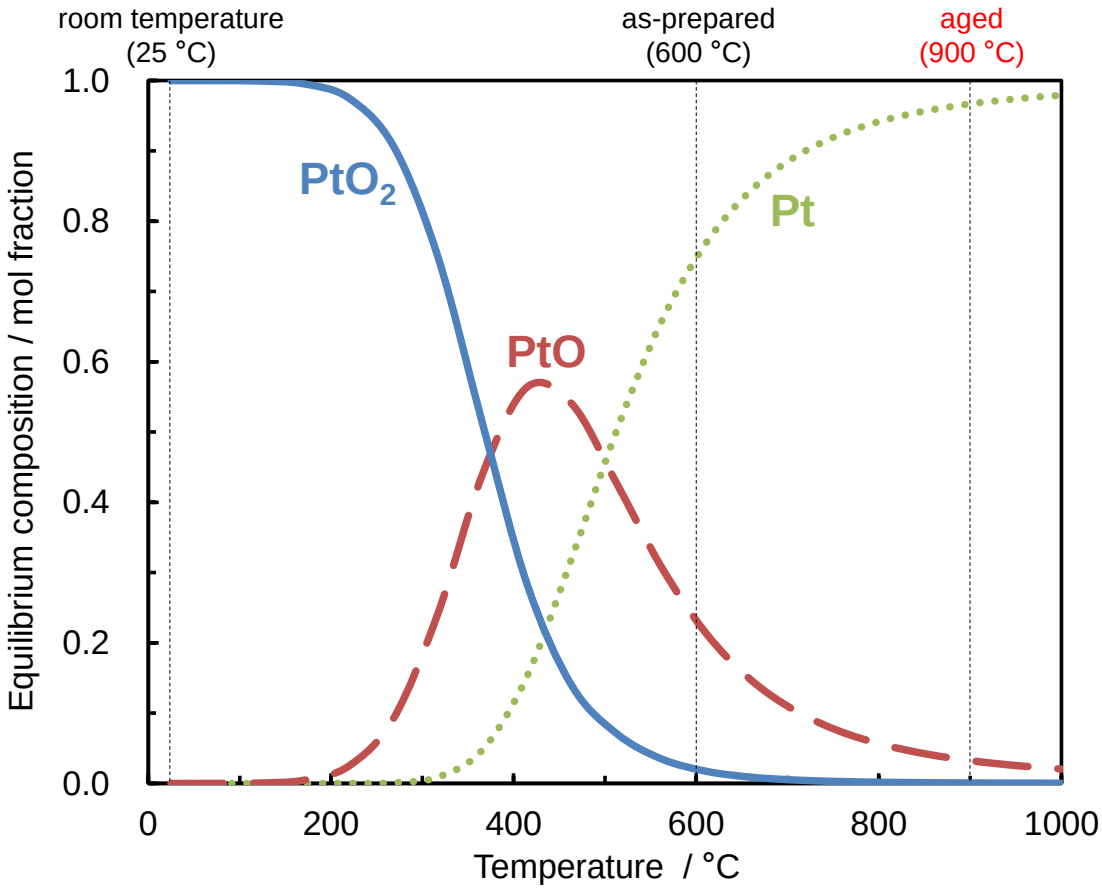


**Figure S1.** Pt−$PtO_x$ phase equilibrium calculated from thermodynamics with HSC Chemistry 9 (Outotec Research Oy, Pori, Finland). Calculation condition: mol fraction of $PtO_{2(s)}$:$O_{2(g)}$:$N_{2(g)}$ = 0.001:20:80, pressure of 1 bar, temperature from 25 to 1000 °C.

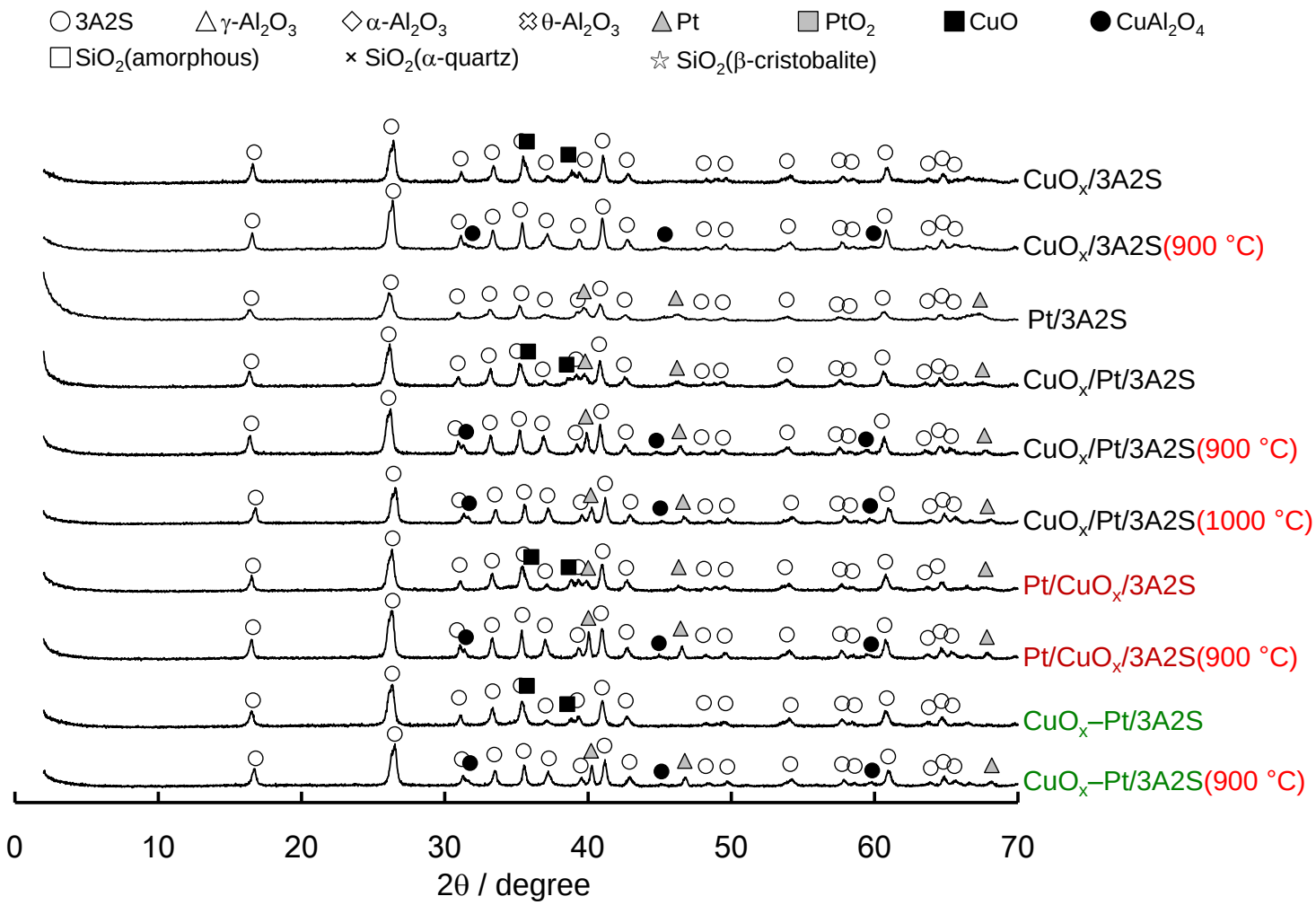


**Figure S2.** XRD patterns of catalysts supported on 3A2S before and after thermal aging 900 °C for 100 h in air.

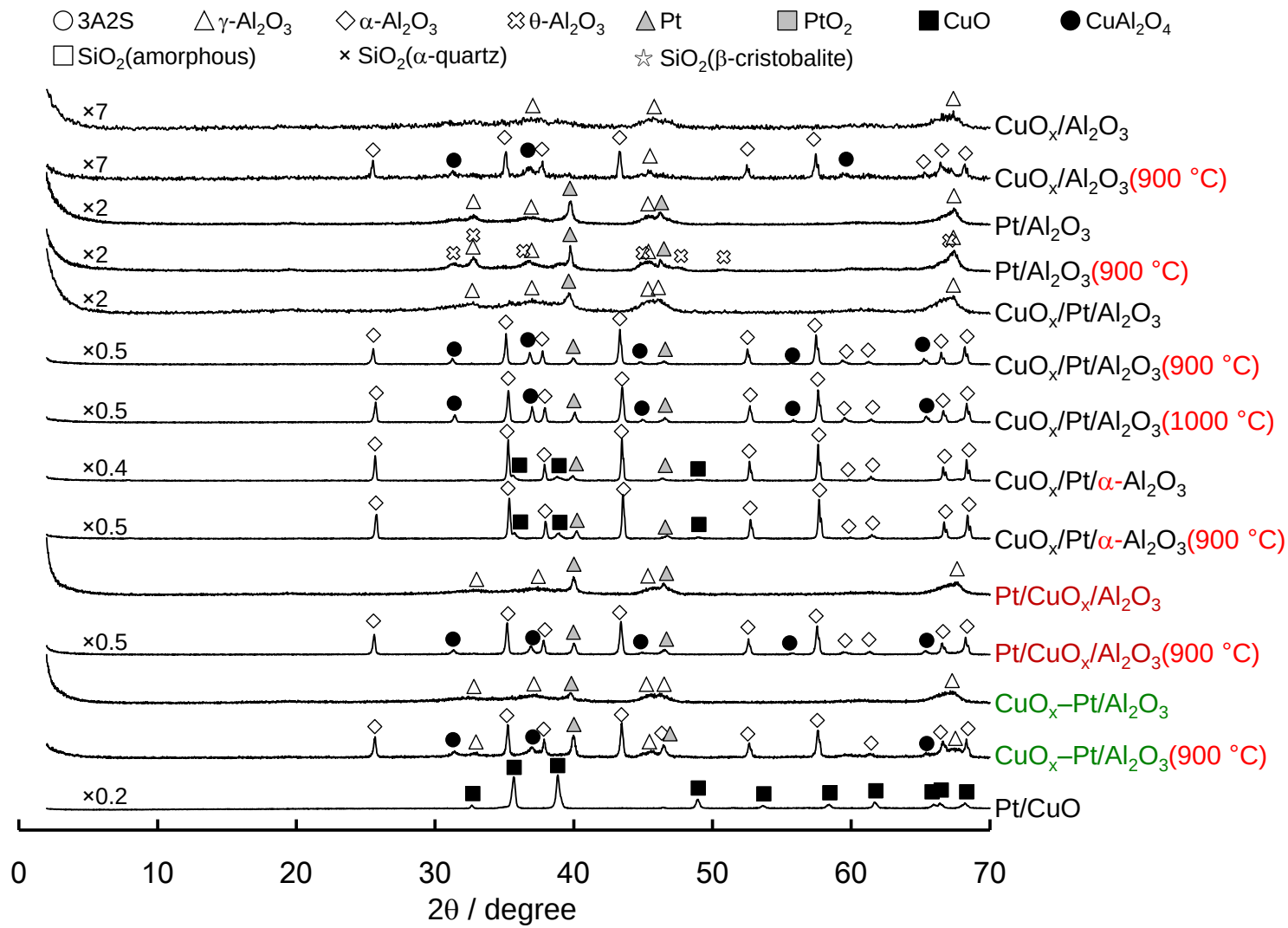


**Figure S3.** XRD patterns of catalysts supported on $Al_2O_3$ and CuO before and after thermal aging 900 °C for 100 h in air.

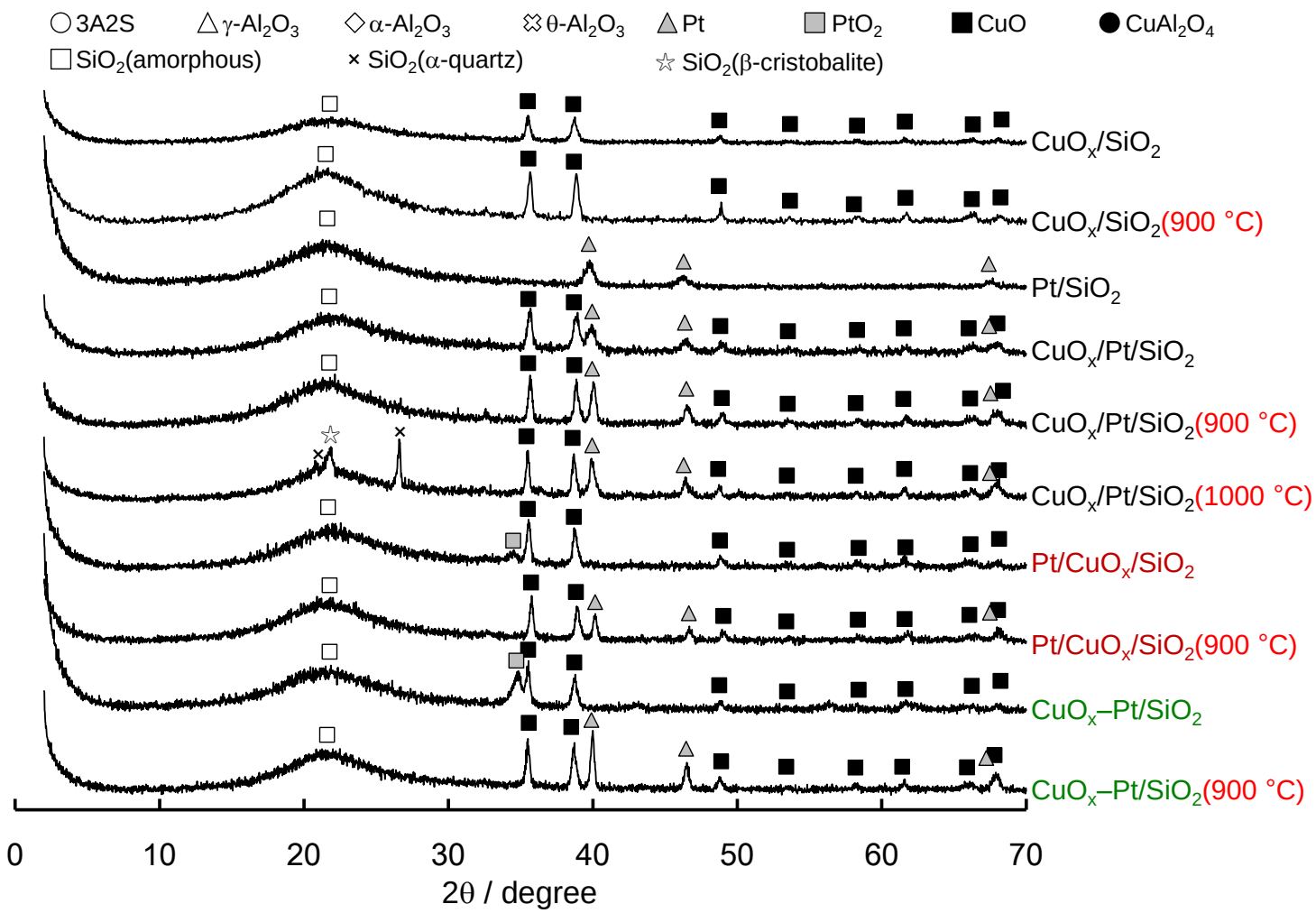


**Figure S4.** XRD patterns of catalysts supported on $SiO_2$ before and after thermal aging 900 °C for 100 h in air.

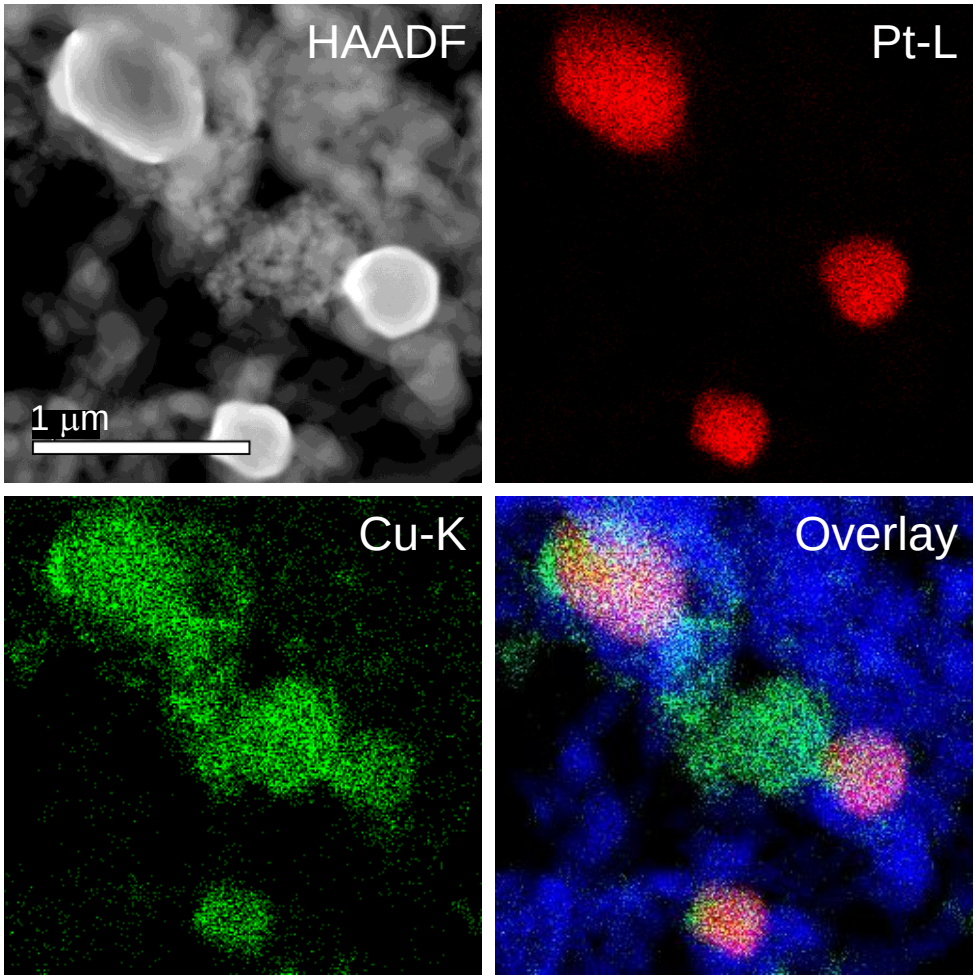


**Figure S5.** HAADF-STEM image and EDS mapping analysis of $CuO_x$/Pt/$SiO_2$(900 °C). Red, green, and blue points denote the Pt-L, Cu-K, and Si-K fluorescence lines.

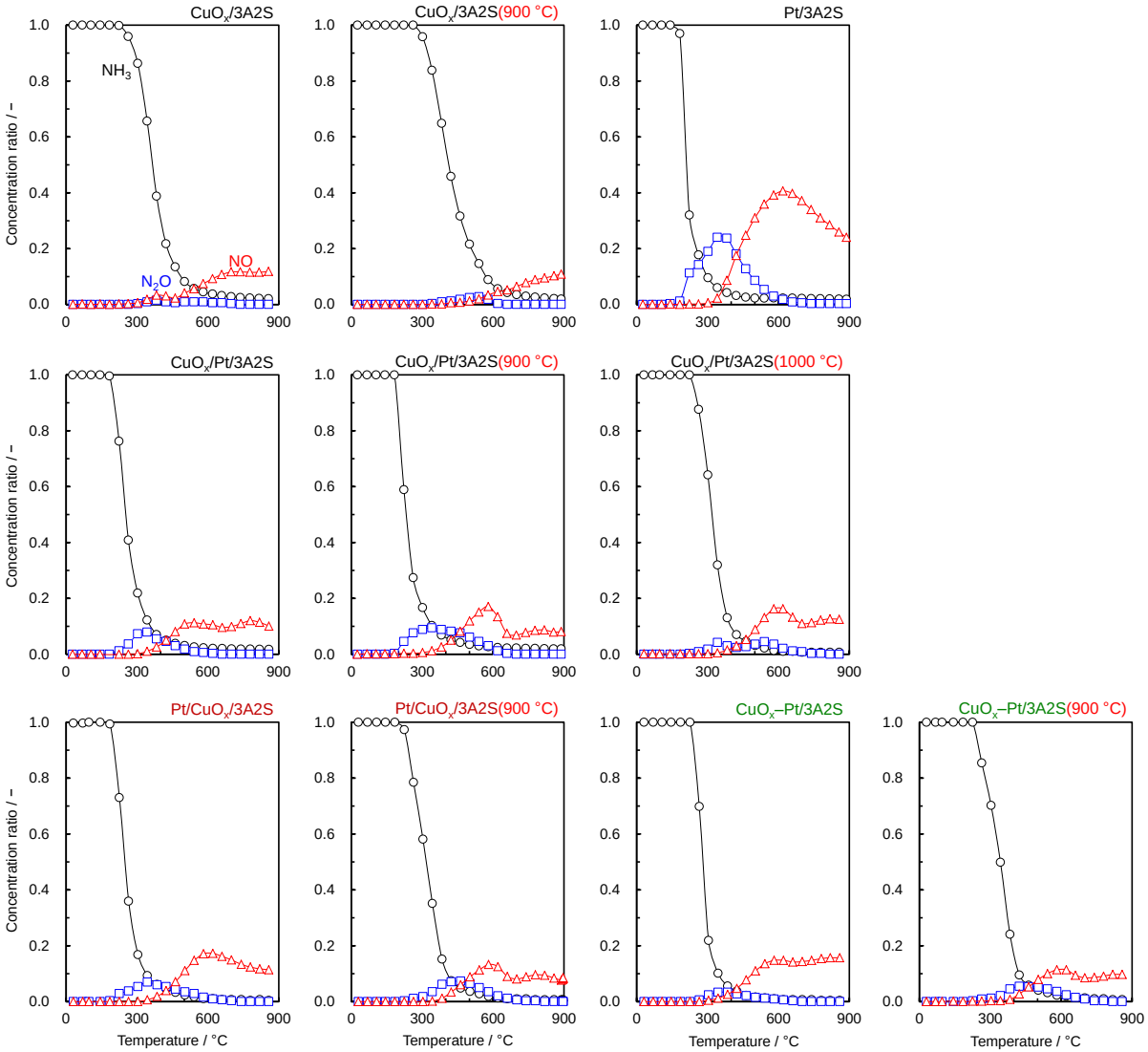


**Figure S6.** Product selectivities for catalytic $NH_3$ combustion over catalysts supported on 3A2S. Reaction conditions: 1.0% $NH_3$, 1.5% $O_2$, $\lambda = 2$, He balance, $W/F = 5.0 \times 10^{-4}$ g min cm$^{-3}$.

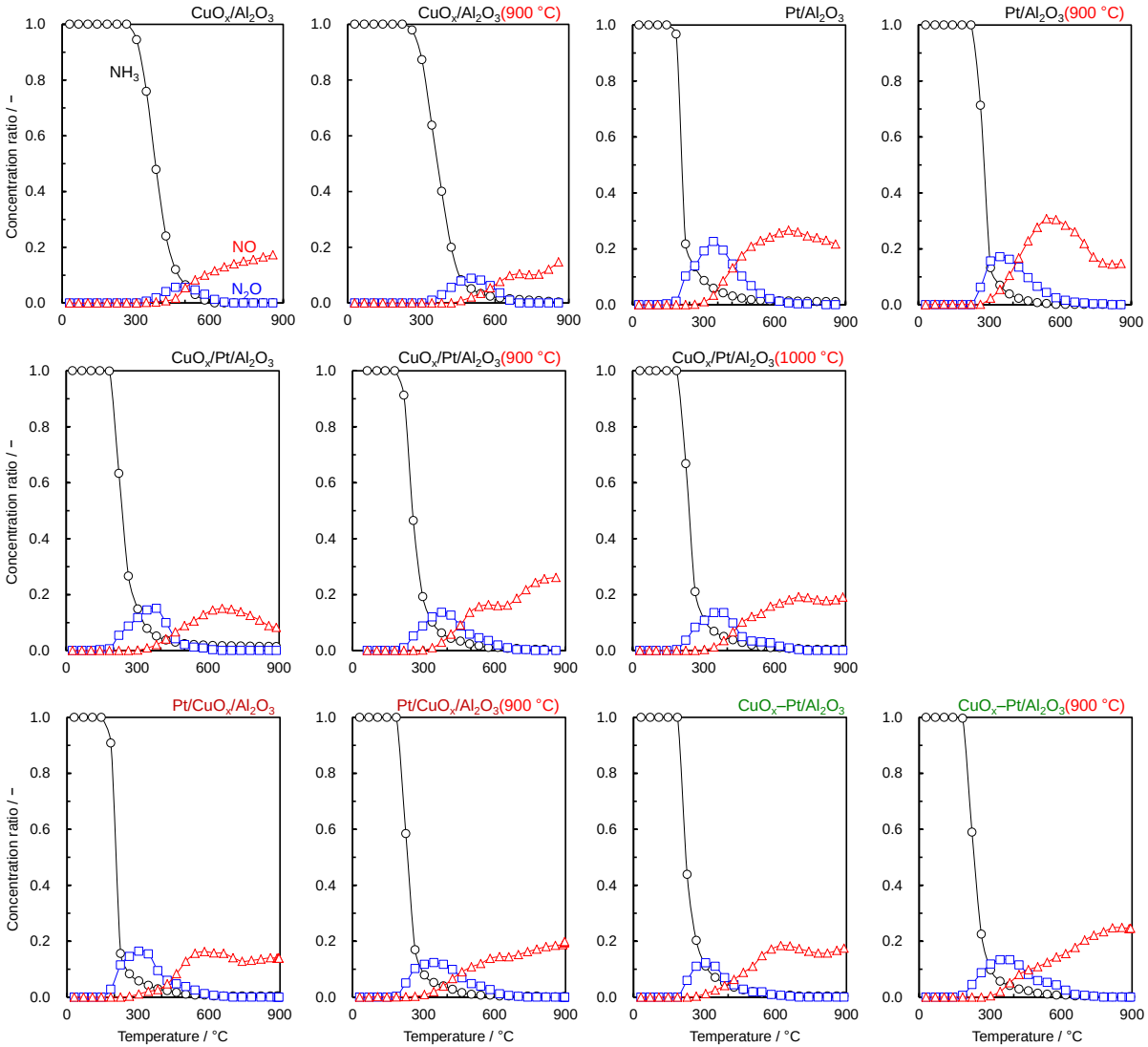


**Figure S7.** Product selectivities for catalytic $NH_3$ combustion over catalysts supported on $Al_2O_3$. Reaction conditions: 1.0% $NH_3$, 1.5% $O_2$, $\lambda = 2$, He balance, $W/F = 5.0 \times 10^{-4}$ g min cm$^{-3}$.

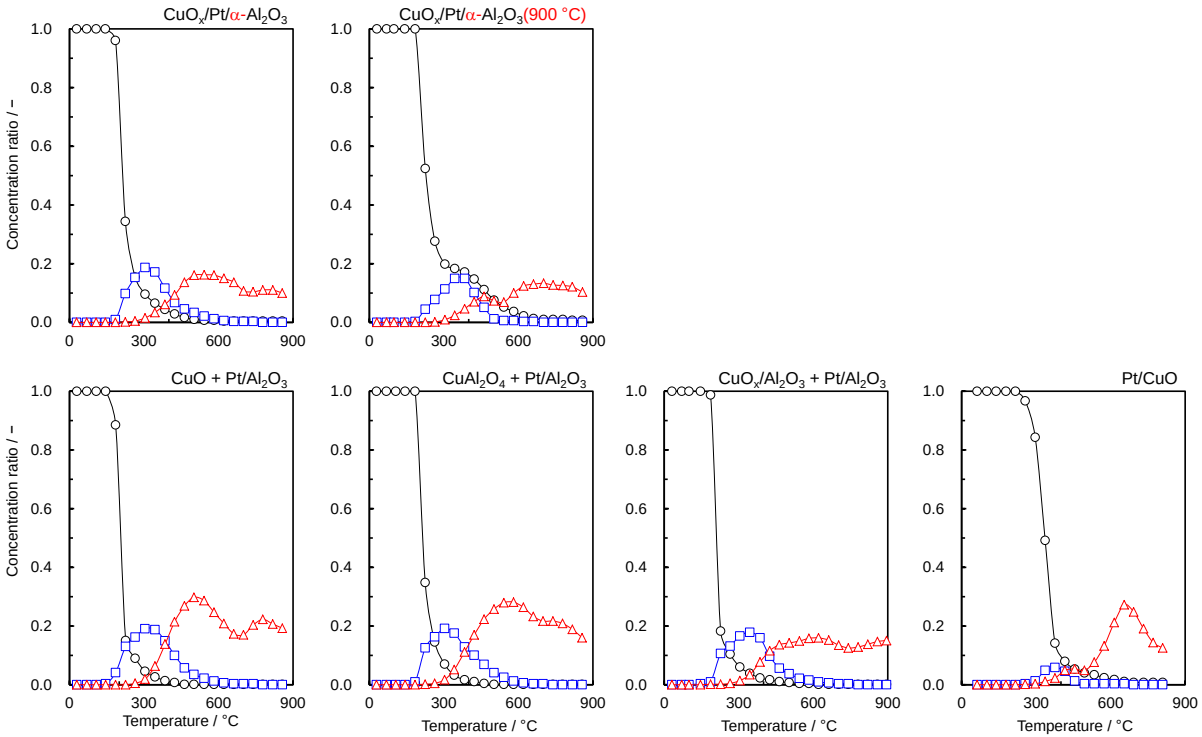


**Figure S8.** Product selectivities for catalytic $NH_3$ combustion over catalysts. Reaction conditions: 1.0% $NH_3$, 1.5% $O_2$, $\lambda = 2$, He balance, W/F = $5.0 \times 10^{-4}$ g min $cm^{-3}$.

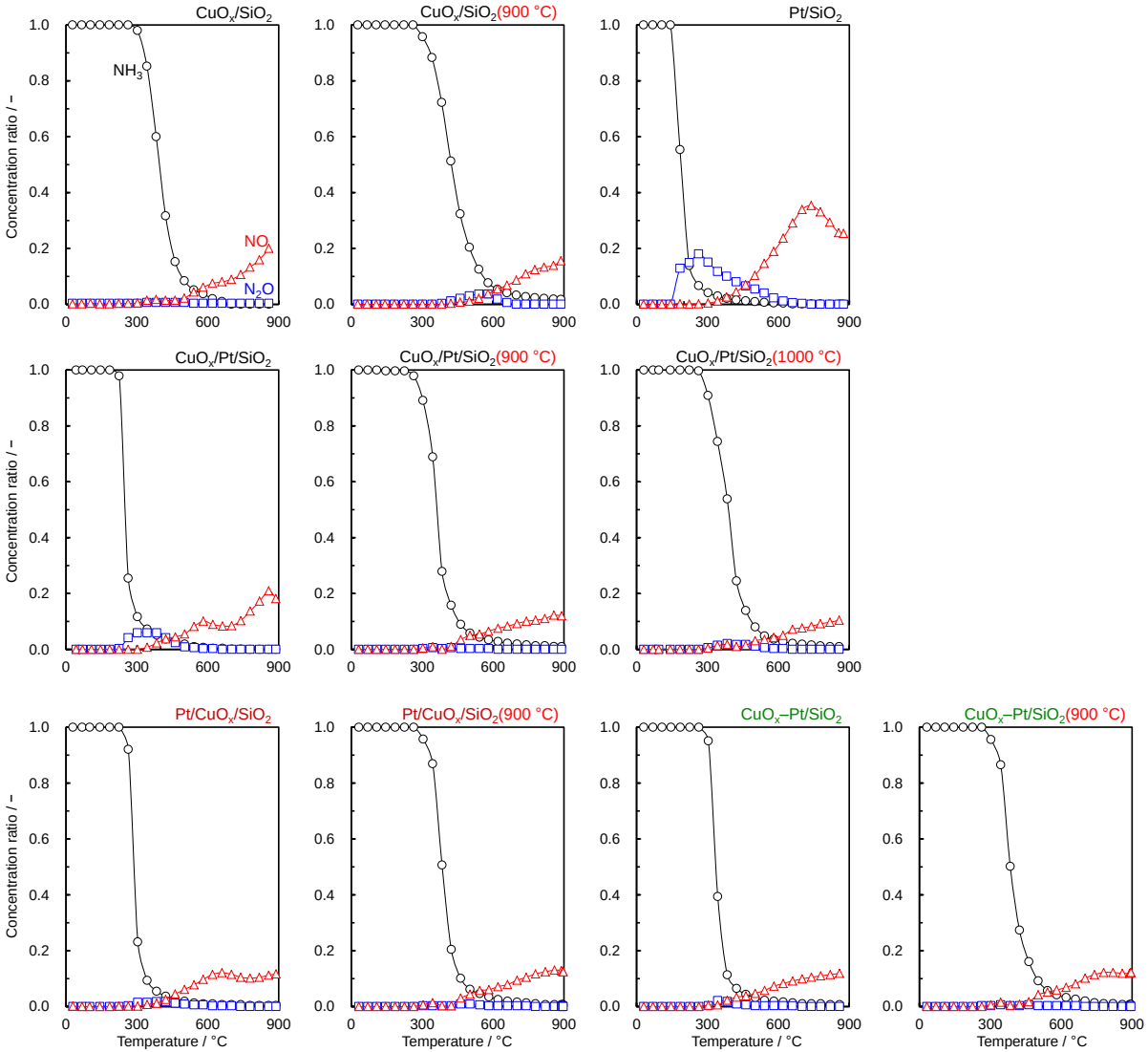


**Figure S9.** Product selectivities for catalytic $NH_3$ combustion over catalysts supported on $SiO_2$. Reaction conditions: 1.0% $NH_3$, 1.5% $O_2$, $\lambda = 2$, He balance, $W/F = 5.0 \times 10^{-4}$ g min cm$^{-3}$.

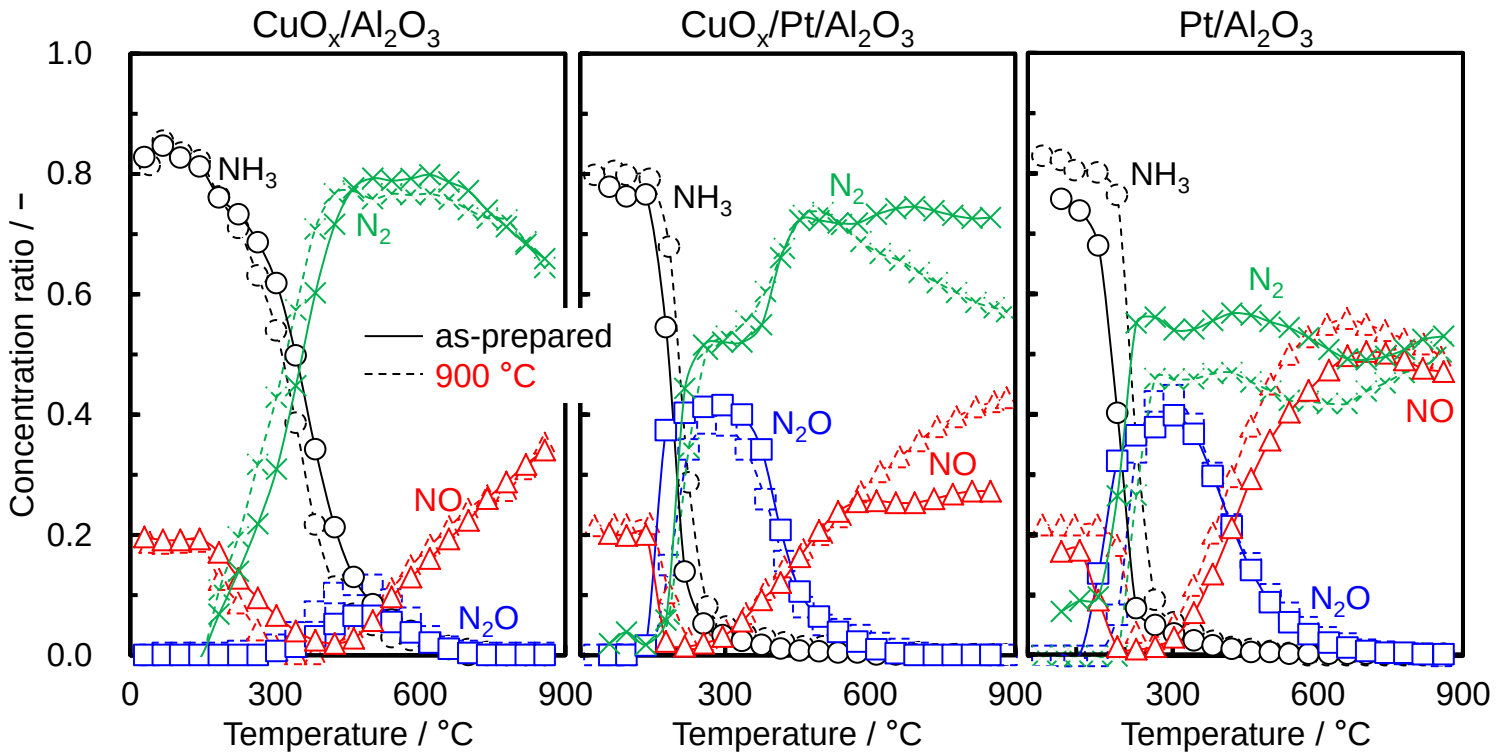


**Figure S10.** Product selectivities for the $NH_3$–NO–$O_2$ reaction over supported catalysts before and after thermal aging. Reaction conditions: 0.8% $NH_3$, 0.2% NO, 1.4% $O_2$, He balance, W/F = $5.0 \times 10^{-4}$ g min $cm^{-3}$.

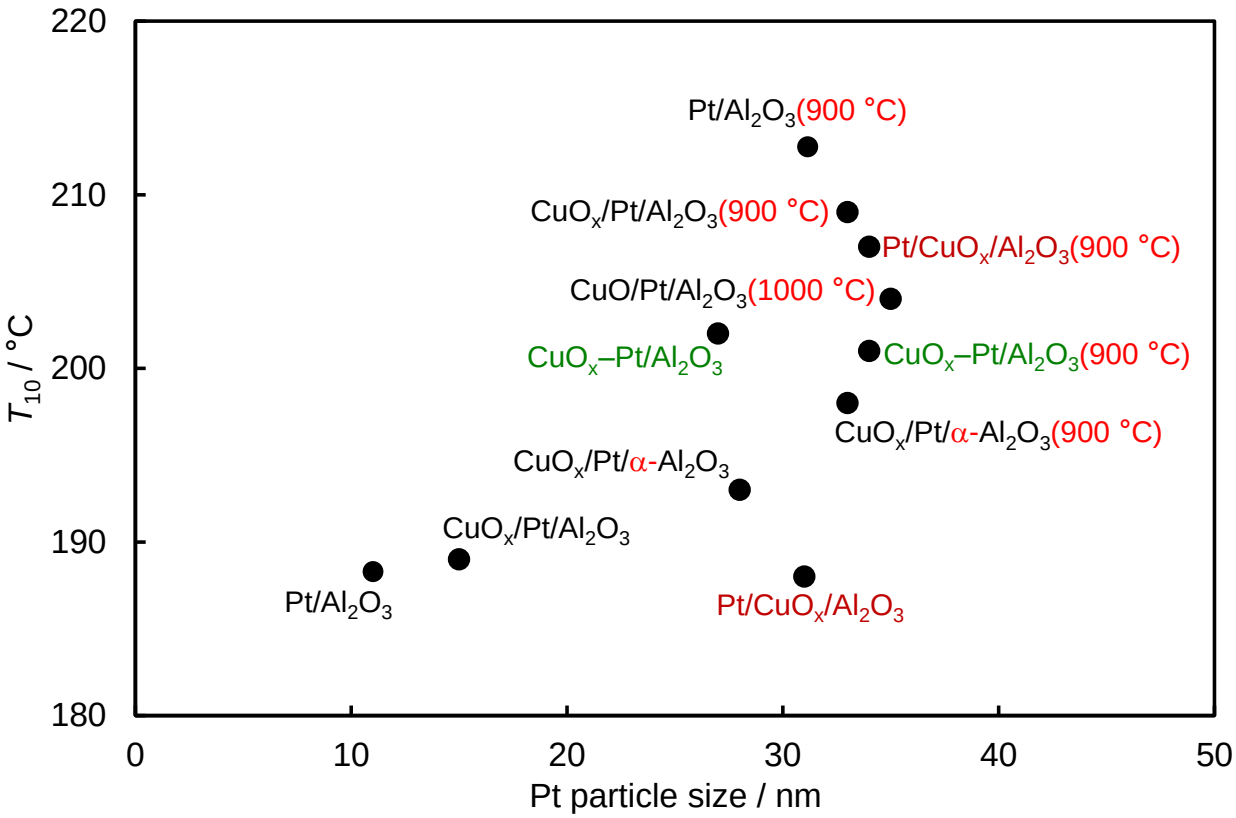


**Figure S11.** Correlation between $NH_3$ combustion activity ($T_{10}$) and Pt particle size for catalysts supported on $Al_2O_3$ before and after thermal aging. Pt particle size was estimated from the XRD line broadening method through the Scherrer equation.

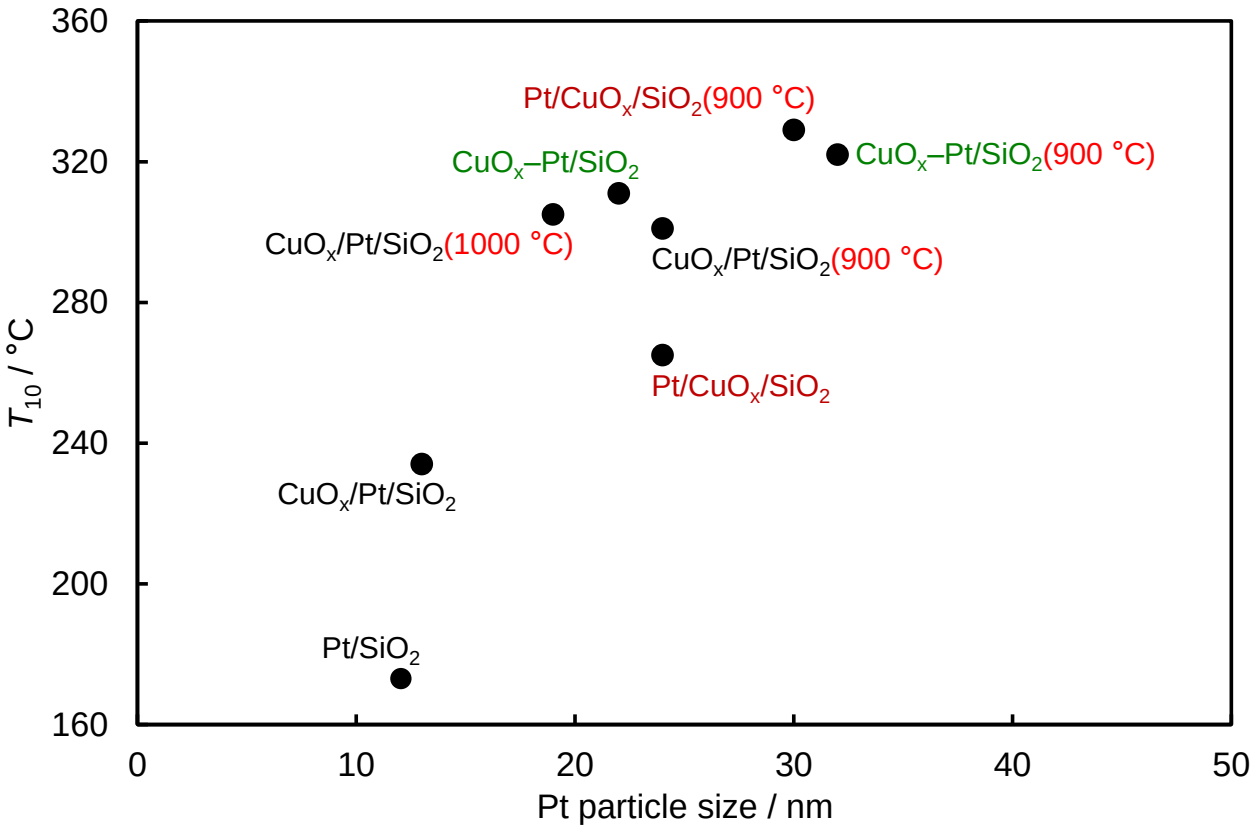


**Figure S12.** Correlation between $NH_3$ combustion activity ($T_{10}$) and Pt particle size for catalysts supported on $SiO_2$ before and after thermal aging. Pt particle size was estimated from the XRD line broadening method through the Scherrer equation.

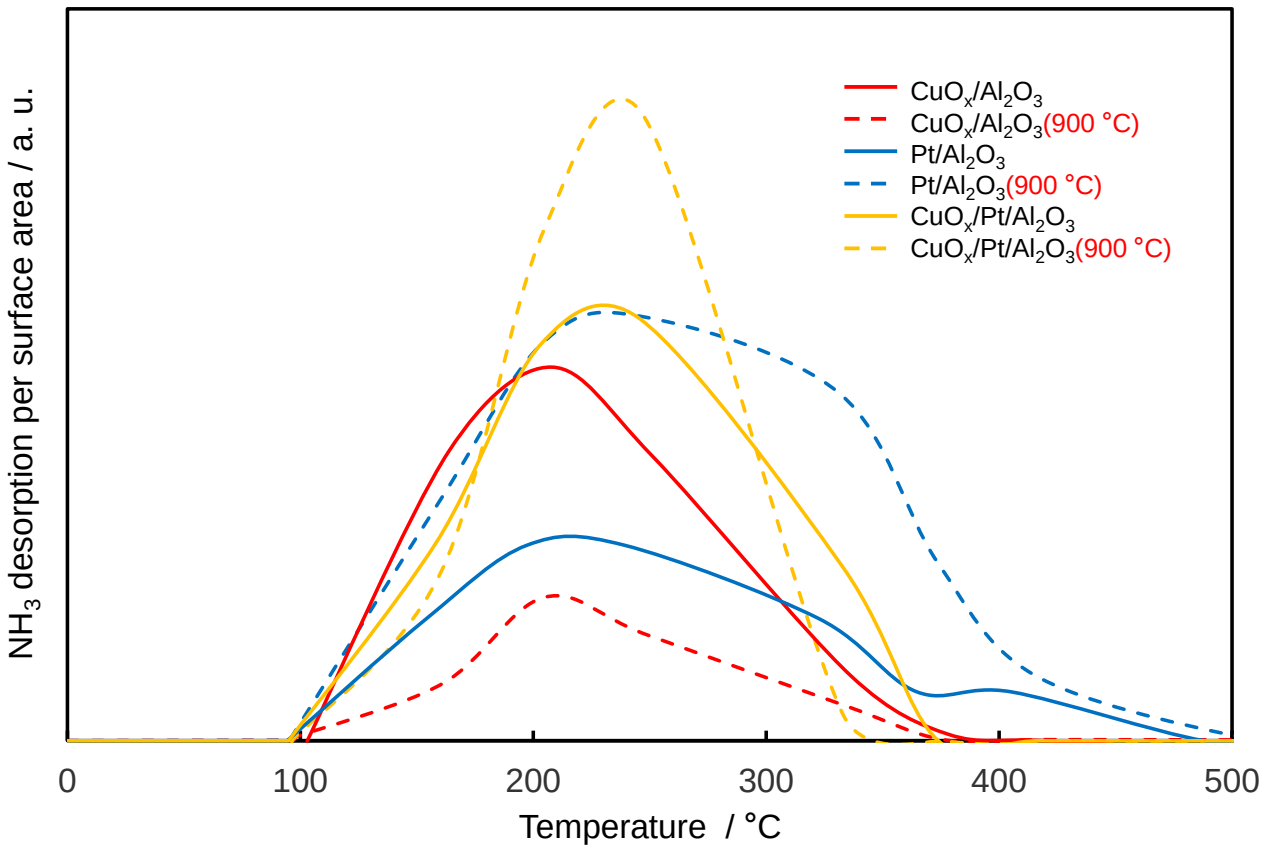


**Figure S13.** $NH_3$-TPD profiles of supported catalysts before and after thermal aging. 5% $NH_3$/He, 10 °C $min^{-1}$, m/z value of 15.

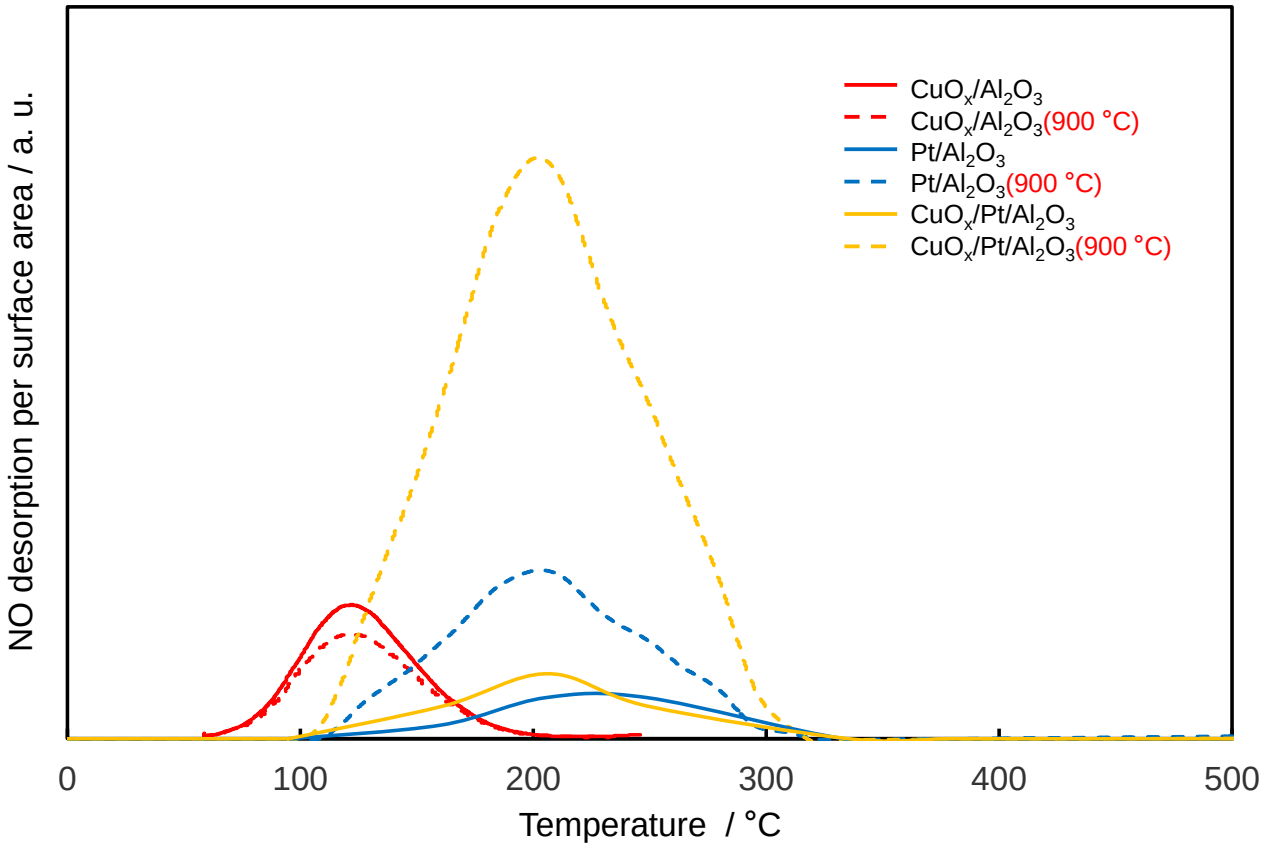


**Figure S14.** NO-TPD profiles of supported catalysts before and after thermal aging. 1% NO/He, 10 °C $min^{-1}$, m/z value of 30.

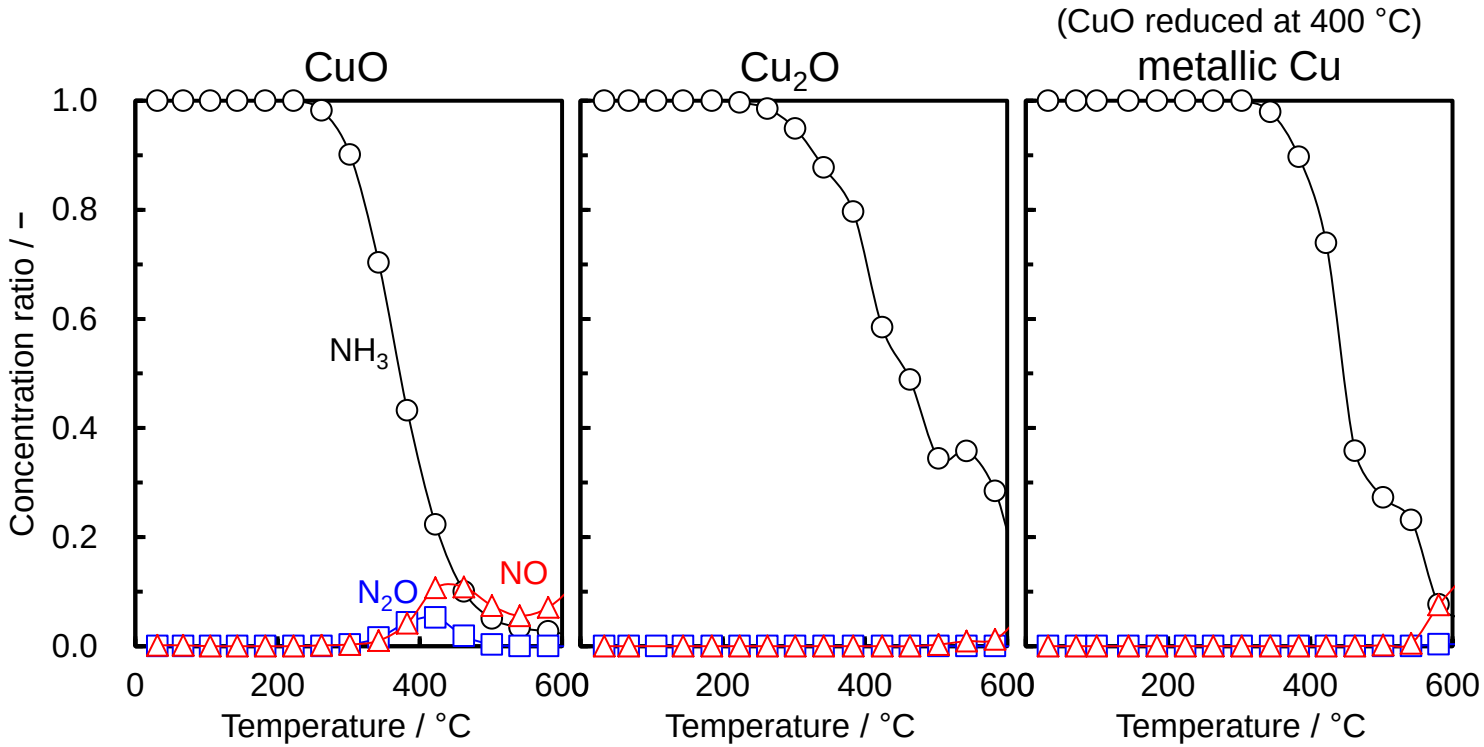


**Figure S15.** Product selectivities for the catalytic combustion of $NH_3$ ($NH_3$–$O_2$) over CuO (Wako Pure Chemicals), $Cu_2O$ (Wako Pure Chemicals), metallic Cu (CuO reduced at 400 °C for 30 min in 5% $H_2$/He). Reaction conditions: 1.0% $NH_3$, 1.5% $O_2$ ($\lambda = 2$), He balance, W/F = $5.0 \times 10^{-4}$ g·min·cm$^{-3}$.

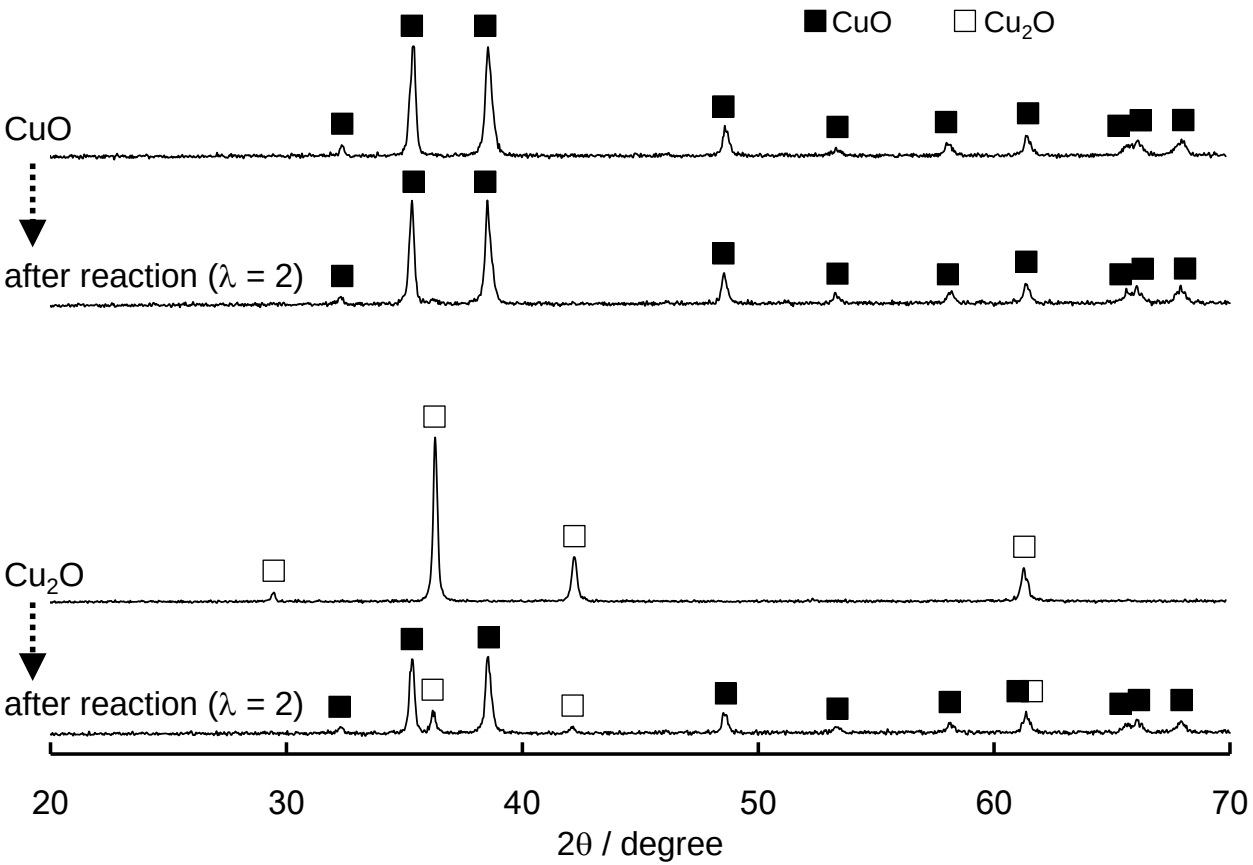


**Figure S16.** XRD patterns of CuO (Wako Pure Chemicals) and $Cu_2O$ (Wako Pure Chemicals) before and after the reaction. Reaction conditions: 1.0% $NH_3$, 1.5% $O_2$ ($\lambda$ = 2.0), He balance and W/F = $5.0 \times 10^{-4}$ g·min·$cm^{-3}$.